

# Electro-mechanical Properties of Carbon Nanotubes

Liu Yang, M. P. Anantram\*, Jie Han and J. P. Lu<sup>a</sup>

*NASA Ames Research Center, Mail Stop T27A-1, Moffett Field, CA, USA 94045-1000*

## Abstract

We present a simple picture to understand the bandgap variation of any chiral carbon nanotubes with tensile and torsional strains. Using this picture, we are able to predict a simple dependence of  $d(\text{Bandgap})/d(\text{strain})$  on the value of  $(N_x - N_y) \bmod 3$ , for semiconducting tubes. We also predict a novel change in sign of  $d(\text{Bandgap})/d(\text{strain})$  as a function of tensile strain arising from a change in the value of the quantum number corresponding to the minimum bandgap. These calculations are complemented by calculations of the change in bandgap using energy minimized structures, and some important differences are discussed.

**Preprint**

The mechanical and electronic properties of carbon nanotubes (CNT) have individually been studied in some detail [1–3] and the predicted dependence of bandgap on chirality [1] has recently been observed. [4] The sensitive dependence of bandgap on chirality leads one to believe that the electronic properties might exhibit interesting dependence on mechanical deformation. This topic is of current importance because the basic ability to manipulate individual nanotubes and apply small strains has been demonstrated. [5] Additionally, it has been speculated that the change in bandgap with mechanical strain may form a basis for applications such as nanoscale electro-mechanical sensors. [6] With regards to the change in electronic properties with mechanical deformation, Refs. [7] and [8] recently studied the effect of uniaxial strain on armchair and zigzag CNT using an analytical Green’s function method based on the  $\pi$  electron approximation and a four orbital numerical method, respectively. Ref. [9], on the other hand predicted the opening of a bandgap in armchair tubes under torsion, by a method that wraps a massless two dimensional Dirac Hamiltonian on a curved surface. In comparison to these studies, we present a simple picture to calculate the variation of bandgap of any chiral nanotube as a function of tensile and torsional strains, with little numerical computation. The main feature that simplifies this is a transformation from a fixed coordinate system to a chirality-dependent coordinate system. We treat the nanotube within the approximation that it is topologically a rolled up graphite sheet and assume a single  $\pi$  orbital per carbon atom.

A uniform graphene sheet has two atoms per unit cell. Upon applying a tensile or torsional strain, while the lattice vectors of the sheet change, the unit cell continues to comprise of two atoms (Fig. 1). Most calculations use the fixed  $(\hat{x}, \hat{y})$  coordinate system to analyze the electronic properties. We however find that transforming to a chirality dependent coordinate system provides a simple picture and hence simplifies the calculation of the electro-mechanical properties. The axes of the chirality dependent coordinate system comprises of the line joining the  $(0,0)$  and  $(N_x, N_y)$  carbon atoms ( $\hat{R}$ ), and the perpendicular ( $\hat{R}_\perp$ ). This coordinate system is preferred because the change in bond vectors can be scaled in a simple manner for tensile and torsional strain. That is, along and perpendicular to the

direction of strain [Eq. (2)].

The fixed and chirality dependent coordinate systems are related by,  $\hat{x} = \sin(\theta)\hat{R} - \cos(\theta)\hat{R}_\perp$  and  $\hat{y} = \cos(\theta)\hat{R} + \sin(\theta)\hat{R}_\perp$ , where,  $\sin(\theta) = \frac{1}{2}\frac{N_x - N_y}{C}$  and  $\cos(\theta) = \frac{\sqrt{3}}{2}\frac{N_x + N_y}{C}$ .  $C = \sqrt{Nx^2 + Ny^2 + NxNy}$ , is the circumference of the tube in units of the equilibrium lattice vector  $a_0$ . The bond vectors between a carbon atom and its three nearest neighbors are represented by  $\vec{r}_1$ ,  $\vec{r}_2$  and  $\vec{r}_3$ , where,

$$\begin{aligned}\vec{r}_1 &= \frac{a_0}{2} \frac{N_x + N_y}{C} \hat{R} - \frac{a_0}{2\sqrt{3}} \frac{N_x - N_y}{C} \hat{R}_\perp + \vec{\delta r}_1 \\ \vec{r}_2 &= -\frac{a_0}{2} \frac{N_y}{C} \hat{R} + \frac{a_0}{2\sqrt{3}} \frac{2N_x + N_y}{C} \hat{R}_\perp + \vec{\delta r}_2 \\ \vec{r}_3 &= -\frac{a_0}{2} \frac{N_x}{C} \hat{R} - \frac{a_0}{2\sqrt{3}} \frac{N_x + 2N_y}{C} \hat{R}_\perp + \vec{\delta r}_3.\end{aligned}\quad (1)$$

For an unstrained graphite sheet, the change in bond vectors  $\vec{\delta r}_i = 0$ . The change in bond vectors are further related by  $\vec{\delta r}_1 = -(\vec{\delta r}_2 + \vec{\delta r}_3)$ .

Within the context of continuum mechanics, application of a small tensile or torsional strain cause approximately the following change in the bond vectors:

$$r_{iR_\perp} \rightarrow (1 + \epsilon)r_{iR_\perp} \quad \text{and} \quad r_{iR} \rightarrow r_{iR} + \tan(\gamma)r_{iR_\perp}, \quad (2)$$

where,  $\epsilon$  is the tensile strain,  $\gamma$  is the shear strain,  $i \in 1, 2, 3$  and  $r_{ip}$  is the  $p$ th component of  $\vec{r}_i$  ( $p \in \hat{R}, \hat{R}_\perp$ ). The component of  $\hat{R}$  ( $\hat{R}_\perp$ ) can also be scaled as a result of tensile (torsional) strain but we neglect this here.

The primary effects of change in bond vectors are to alter the hopping parameter between carbon atoms and lattice vectors of the unit cell. The hopping parameter of bond  $i$  is represented by  $t_i$  and is assumed to scale with the bond length as,  $t_i = t_0 r_0/r_i^2$ . [7,8] We then derive that the band structure of the strained graphene sheet, within  $sp^2$  approximation is, [10]

$$\begin{aligned}E(k_\perp) &= (t_1^2 + t_2^2 + t_3^2 + 2t_1t_2 \cos[\pi q \frac{Nx + 2Ny}{C} - \frac{\sqrt{3}}{2} \frac{Nx}{C} k_\perp a_0 + \vec{k} \cdot (\vec{\delta r}_1 - \vec{\delta r}_2)] \\ &\quad + 2t_1t_3 \cos[\pi q \frac{2Nx + Ny}{C} + \frac{\sqrt{3}}{2} \frac{Ny}{C} k_\perp a_0 + \vec{k} \cdot (\vec{\delta r}_1 - \vec{\delta r}_3)] \\ &\quad + 2t_2t_3 \cos[\pi q \frac{Nx - Ny}{C} + \frac{\sqrt{3}}{2} \frac{Nx + Ny}{C} k_\perp a_0 + \vec{k} \cdot (\vec{\delta r}_2 - \vec{\delta r}_3)])^{\frac{1}{\sqrt{2}}}\end{aligned}\quad (3)$$

where,  $\vec{k} = k\hat{R} + k_{\perp}\hat{R}_{\perp}$ . The condition for quantization of the k-vector along the circumferential direction,  $kCa = 2\pi q$  has been used in deriving Eq. (3). The band structure of any  $(N_x, N_y)$  tube in the presence of tensile or torsional strain can be easily calculated from Eqs. (2) and (3). Using such a procedure, we find that for semiconducting tubes independent of chirality, **(i)** while  $|dE_g/d\sigma|$  are largest and smallest for zigzag and armchair tubes respectively under tension, the *opposite* is true under torsion. For chiralities in between, the general trend is that  $|dE_g/d\sigma|$  changes gradually from the armchair to the zigzag values [Figs 2 and 3]. **(ii)** the sign of  $dE_g/d\sigma$  is given by  $(N_x - N_y) \bmod 3$  [11] for both tension and torsion [Figs. 2 and 3]. **(iii)** as tensile strain increases, a sudden reversal in the sign of  $dE_g/d\sigma$  becomes possible. This corresponds to a change in the value of  $q$  corresponding to the band with minimum energy, as illustrated later.

We believe that these results are significant because prior work considered only the highly symmetric armchair and zigzag tubes. Moreover, our procedure is considerably simpler than it can handle chiral tubes with ease. These findings have further been verified by four orbital calculations and the results do not change qualitatively.

The above picture assumed a simple form (continuum mechanics) for the scaling of bond lengths as a function of strain [Eq. (2)] and did not account for the change in bond lengths due to curvature. An important issue is the validity of the above results when energy minimized structures are considered. So, we compute the bandgap using  $\delta r_i$  obtained by an energy minimization procedure and compare the results to that obtained from continuum mechanics. The energy minimization procedure uses Brenner potential [12] and periodic boundary conditions. As regards the topology, the primary input to the code that we have developed [13], is the length of the structure. The radius, bond lengths and angles evolve to the configuration of minimum energy for the fixed length. This energy minimized structure is the input to a code that calculates the density of states using the method discussed in Ref. [14]. The results obtained by this numerically more extensive method are qualitatively similar to the above findings for semiconducting and armchair tubes [13]. An interesting

exception in the case of torsion is discussed below. For other metallic/semi-metallic tubes, the symmetry in the bond vectors is lost when energy minimization is performed. As a result, it is known that the bandgap is no longer zero but has a small finite value. Then, we find that applying a strain usually causes a transition to a metallic state, even for chiral tubes. One such case is discussed. In the remainder of this paper, we focus on armchair and zigzag tubes, deriving simpler expression that illustrate the physics more directly.

The band structure of zigzag tubes under tension is given by (from Eq. (3)),

$$E(k_{\perp}) = \pm t_1 \left[ 1 \pm \left( \frac{4t_2}{t_1} \right) \cos\left(\frac{q\pi}{N}\right) \cos(k_{\perp} b_{zz}) + \left( \frac{2t_2}{t_1} \right)^2 \cos^2\left(\frac{q\pi}{N}\right) \right]^{\frac{1}{2}}, \quad (4)$$

where,  $b_{zz} = r_{1R} - r_{2R}$  [Fig. 1] and  $t_2 = t_3$ , as a result of symmetry. The minimum of  $E(k_{\perp})$  occurs at  $k_{\perp} = 0$ ,

$$E_{k_{\perp}=0} = \pm t_1 \left| 1 - \frac{2t_2}{t_1} \cos\left(\frac{q\pi}{N}\right) \right|. \quad (5)$$

While Eq. (5) is compact, we find that expanding it to first order in  $\delta r_i$  is useful to understand the features of  $dE_g/d\sigma$  seen in Fig. 1 for semiconducting zigzag tubes. To first order in  $\delta r_i$ , [15]

$$E(0) = E_0(q) - 2t_0 \frac{\delta r_1}{r_0} \left[ 1 - \frac{2\delta r_2}{\delta r_1} \cos\left(\frac{q\pi}{N}\right) \right] \text{sgn}(x), \quad (6)$$

where,  $\text{sgn}(x) = [1 - 2\cos(q\pi/N)]$ . The minimum of  $E_0(q) = t_0 |1 - 2\cos(q\pi/N)|$  is half of the bandgap of an unstrained tube. Eq. (6) is central to understanding the slope of  $dE_g/d\sigma$  as a function of  $N$  and the following interesting features follow: **(a)** Owing to the bond orientations, it is expected that for small values of strain,  $\delta r_1 > \delta r_2$ . The factor  $2\cos(q\pi/N)$  is approximately equal to  $1 \mp 1/(3\sqrt{3}q)$  for  $N = 3q \pm 1$ . Then as seen in Fig. 1, we obtain that the sign of linear response  $dE_g/d\sigma$  is negative for  $N = 3q - 1$  and positive for  $N = 3q + 1$ , independent of tube diameter (Fig. 2). [7,8] When bond lengths from continuum mechanics are used, we find that  $|dE_g/d\sigma| \approx 3t_0$ , for small values of strain (see zigzag cases in Fig. 2). **(b)** The first term of Eq. (6) takes the smallest possible value for  $q = q_0$  that satisfies  $N = 3q_0 \pm 1$ . The second term can however abruptly change sign when  $q$  changes from

$q_0$  to  $q_0 \pm 1$ . As a result, a dramatic change in the sign of  $dE_g/d\sigma$  becomes possible if the magnitude of the second term is larger than the change in the first term (Fig. 4). That is, as a function of strain, the quantum number  $q$  that yields minimum energy in the conduction band can change and this is accompanied by an abrupt change in the sign of  $dE_g/d\sigma$ . It can also be shown easily that the strain required to observe this effect decreases approximately as the inverse radius of the tube for large  $N$ . This is illustrated by comparing the (10,0) and (19,0) tubes in Fig. 4. The inset of Fig. 4 shows the movement of the  $q=6$  and  $q=7$  bands for the (19,0) tube for different values of strain. They move in opposite directions with increase in strain, leading to the discussed cross over. **(c)** For semi-metallic zigzag tubes  $(3q,0)$ , from Eq. (5,  $E_g = |t_1 - t_2| = 2t_0 \frac{|\delta r_1|}{r_0} |1 - \frac{\delta r_2}{\delta r_1}|$  (to first order  $\delta r_i$ ). This results in a small non zero band gap (Fig. 4) of these tubes as predicted before. [7,16] However, our results indicate that the bandgap decreases to zero as a result of stretching rather than compression, as found in Ref. [7]. This follows because the bond lengths differ in the following manner as a result of energy minimization: For a rolled graphene sheet (without energy minimization), it is easy to see that  $r_2 < r_1$ . Upon energy minimization, we find that  $r_2 > r_1$ . Then, stretching initially causes the two bond lengths to become comparable and as a result, the bandgap approaches zero (is equal to zero when  $r_2 = r_3 = r_1$ ). The bandgap increases on stretching further as  $r_1 > r_2$ . Our energy minimization simulations show that  $r_2/r_1$  decreases with increase in tube diameter. It would be of interest to see if  $r_2 < r_1$  for larger diameter tubes. This would result in a change in sign of  $dE_g/d\sigma$  above a threshold diameter, in the case of  $(3q,0)$  tubes.

Under the influence of a tensile strain, the change in bond vectors of armchair tubes are:  $\vec{\delta r}_1 = \delta r_{1R} \hat{R}$ ,  $\vec{\delta r}_2 = \delta r_{2R} \hat{R} + \delta r_{2R_\perp} \hat{R}_\perp$  and  $\vec{\delta r}_3 = \delta r_{2R} \hat{R} - \delta r_{2R_\perp} \hat{R}_\perp$ . Further,  $t_2 = t_3$  because of symmetry between bonds 2 and 3 [Fig. 1]. The boundary condition along the circumferential direction is given by  $kN|\vec{r}_1 - \vec{r}_2|_R = 2\pi q$ . Using this information in Eq. (3), we obtain the following  $E(k_\perp)$  relationship for armchair tubes,

$$E(k_\perp) = \pm t_1 \left[ 1 \pm \left( \frac{4t_2}{t_1} \right) \cos\left(\frac{q\pi}{N}\right) \cos\left(\frac{k_\perp b_{ac}}{2}\right) + \left( \frac{2t_2}{t_1} \right)^2 \cos^2\left(\frac{k_\perp b_{ac}}{2}\right) \right]^{\frac{1}{2}}, \quad (7)$$

where,  $b_{ac} = r_{2R_\perp} - r_{3R_\perp}$ . The band that crosses the zero of energy corresponds to  $q = N$  and  $k_\perp b_{ac} = \pm 2\pi/3$ . In the presence of tensile strain, the  $E(k_\perp)$  relationship of this band is,

$$E(k_\perp)|_{q=N} = \pm 2t_1 \left| \frac{t_2}{2t_1} - \cos\left(\frac{k_\perp b_{ac}}{2}\right) \right|. \quad (8)$$

Note that when  $k_\perp = 2b_{ac}^{-1}\text{acos}(t_2/2t_1)$ , the bandgap is zero. That is, the bandgap of an armchair tube remains zero in the presence of tensile strain; the  $k$  vector corresponding to zero bandgap however depends on the strain and is no longer  $\pm 2\pi/3$ . This is an interesting difference from zigzag tubes, where the band minimum continues to be at  $k = 0$  in the presence of strain.

We now proceed to discuss the change in bandgap as a result of torsional strain. Torsion breaks the symmetry between bonds 2 and 3, and the three bonds of a carbon atom change by different amounts [Fig. 1]. We find from Eq. (3) that for semiconducting zigzag tubes, to first order in  $\delta r_i$ , [15]

$$E(0) = E_0(q) - 2t_0 \frac{1}{r_0} \left[ \delta r_1 - (\delta r_2 + \delta r_3) \cos\left(\frac{q\pi}{N}\right) \right] \text{sgn}(x). \quad (9)$$

From Fig. 1, it easy to see that  $\delta r_2$  and  $\delta r_3$  change in opposite directions under torsion. As a result, they have compensating effects on the change in bandgap [Eq. (9)]. Using the bond lengths computed from continuum mechanics [Eq. (2)], we find that the magnitude of  $dE_g/d\sigma$  is small and that the sign of the slope is equal to  $N \bmod 3$ . As expected, this also follows from Eq. (9) when the bond length changes from continuum mechanics are used. In constrast, the sign of  $dE_g/d\sigma$  is opposite to the continuum mechanics result, when bond lengths obtained from energy minimization are used. We find that for small strains, the factor  $\left[ \delta r_1 - (\delta r_2 + \delta r_3) \cos\left(\frac{q\pi}{N}\right) \right]$  is a small negative number, instead of the small postivie number that continuum mechanics yields. Future work to verify this result using alternate methods would be useful.

In comparison to the case of zigzag tubes, the effect of torsion is dramatic on armchair tubes. For the  $q = N$  band, it follows from Eq. (3) that,

$$E_{q=N}(k_\perp) = t_1^2 + t_2^2 + t_3^2 + 2t_1 t_2 (2\cos^2\left(\frac{k_\perp a}{2}\right) - 1) + 2(t_1 + t_2)t_3 \cos\left(\frac{k_\perp a}{2}\right). \quad (10)$$

The minimum bandgap is obtained by minimizing Eq. (10) with respect to  $\cos(\frac{k_{\perp}a}{2})$ . We find that the band minima has moved away from  $k_{\perp}b_{ac} = \pm 2\pi/3$  and a finite bandgap equal to,

$$E_g = 2|t_2 - t_3| \sqrt{1 - \frac{t_1^2}{4t_2t_3}} \approx 2t_0 \frac{|\delta r_2 - \delta r_3|}{r_0} \sqrt{3 - \frac{2\delta r_1 - \delta r_2 - \delta r_3}{2r_0}}. \quad (11)$$

develops. The opposite signs of change in lengths of bonds 2 and 3 [Fig. 1] aid in making  $dE_g/d\sigma$  large, in comparison to zigzag tubes. The new bond lengths of the graphene sheet to first order in  $\delta R$  [Fig. 1] are  $r_1 = a/\sqrt{3}$ ,  $r_2 = a/\sqrt{3} + \delta R/4$  and  $r_3 = a/\sqrt{3} - \delta R/4$ . Substituting these values in Eq. (11),  $E_g = \sqrt{3}t_0\delta R/r_0 = 3t_0\gamma$  (see armchair case in Fig. 3), where  $\gamma$  is the shear strain. [9]

In conclusion, we present a simple picture to predict the  $E_g$  versus  $\sigma$  behavior of CNT tubes of arbitrary chirality. We find that under tensile strain,  $|dE_g/d\sigma|$  of zigzag tubes is  $3t_0$  independent of diameter, and continually decreases as the chirality changes to armchair, when it takes the value zero. The sign of  $dE_g/d\sigma$  follows the  $(N_x - N_y) \bmod 3$  rule. In contrast, we show that under torsional strain,  $|dE_g/d\sigma|$  of armchair tubes is  $3t_0$  independent of diameter, and continually decreases as the chirality changes to zigzag, where it takes a small value. The sign of  $dE_g/d\sigma$  is predicted to follow the  $(N_x - N_y) \bmod 3$  rule. We also predict a change in the sign of  $dE_g/d\sigma$  as function of strain, corresponding to a change in the value of  $q$  that corresponds to the bandgap minimum.



## REFERENCES

- \* anant@nas.nasa.gov; Author to whom correspondence is to be addressed.
- <sup>a</sup> Permanent address: CB 3255 Phillips Hall, University of North Carolina - Chapel Hill, Chapel Hill, NC 27599;
- [1] M. S. Dresselhaus et. al, Chap. 19 of Science of Fullerenes and Carbon Nanotubes, Academic Press, (1996).
- [2] M. B. Nardelli et al., Phys. Rev. B **57** 4277 (1998)
- [3] J. Lu and J. Han, "Carbon nanotubes and nanotube based nanodevices" in Quantum-based electronic devices and systems, edited by P. K. Tien et. al. (World Scientific publishing, Singapore, 1998)
- [4] J. W. G. Wildoer et. al, Nature **391**, 59 (1998) and T. W. Odom et. al, Nature **391**, 62 (1998).
- [5] L. C. Venema et. al, Nature **391**, 62 (1998) and T. Hertel et. al, Journal of Physical Chemistry B **102**, 910 (1998).
- [6] C. Joachim et. al, Phys. Rev. Lett. **74**, 2102 (1995)
- [7] R. Heyd et. al, Phys. Rev. B **55**, 6820 (1997).
- [8] D. W. Brenner, Private Communication.
- [9] C. L. Kane and E. J. Mele, Phys. Rev. Lett **78**, 1932 (1997).
- [10] This expression can be obtained by a simple extension of P. R. Wallace, Phys. Rev. **71**, 622 (1947).
- [11] defined in terms of  $\{-1, 0, 1\}$ ; i.e.,  $(N_x - N_y) \bmod 3$  equal to 0, 1 and 2 corresponds to 0, 1, and -1 respectively in the notation used.
- [12] D. W. Brenner Phys. Rev. B **42**, 9458 (1990)

- [13] Liu Yang et. al, Unpublished.
- [14] M. P. Anantram and T. R. Govindan, Phys. Rev. B **58**, no. 7 (1998).
- [15]  $2t_0\delta r_i$  can be replaced by  $\delta t_i$  in this expression.
- [16] S.G. Louie, in Proceedings of the Robert A. Welch Foundation 40th Conference on Chemical Research, Houston, 1996 (Welch Foundation, Houston, 1996).

## Figure Captions:

Fig. 1: The fixed  $(x, y)$  and chirality  $(R, R_\perp)$  dependent coordinates.  $r_1, r_2$  and  $r_3$  correspond to bonds 1, 2 and 3 respectively.  $\vec{b}_1$  and  $\vec{b}_2$  are the lattice vectors of the two dimensional sheet.

Fig. 2: Bandgap versus tensile strain: The solid, dashed and dotted lines correspond to  $(N_x - N_y) \bmod 3$  values of 1, -1 and 0 respectively.

Fig. 3: Bandgap versus torsional strain: The solid, dashed and dotted lines correspond to  $(N_x - N_y) \bmod 3$  values of 1, -1 and 0 respectively.

Fig. 4: Bandgap versus uniaxial strain: The change in slope of the (10,0) and (19,0) tubes around 10% and 5% strain respectively is due to a change in the quantum number  $q$  that yields the minimum bandgap. Inset: E vs k of the q=7 (solid) and q=6 (dashed) bands as a function of strain. Strains of 0%, 3% and 6% correspond to increasing thickness of the lines. The (8,0) torsion curve has been shifted by  $-0.12$  units. The slope of the torsion curves is opposite of that in Fig. 3.

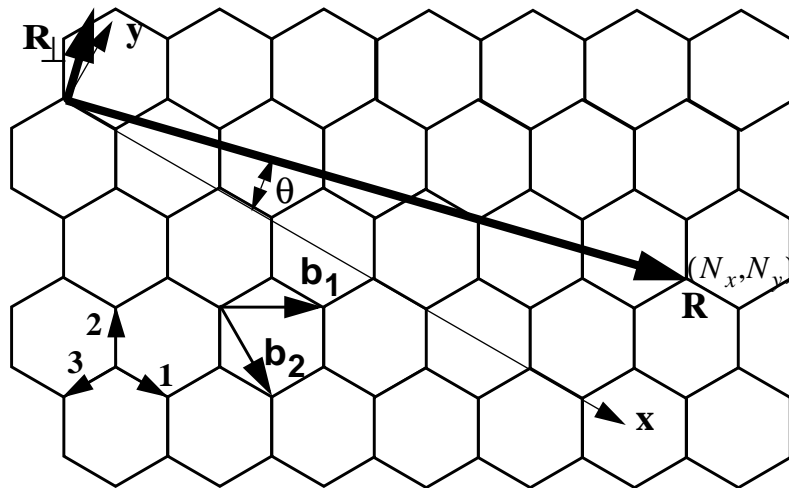


Fig. 1 / Yang

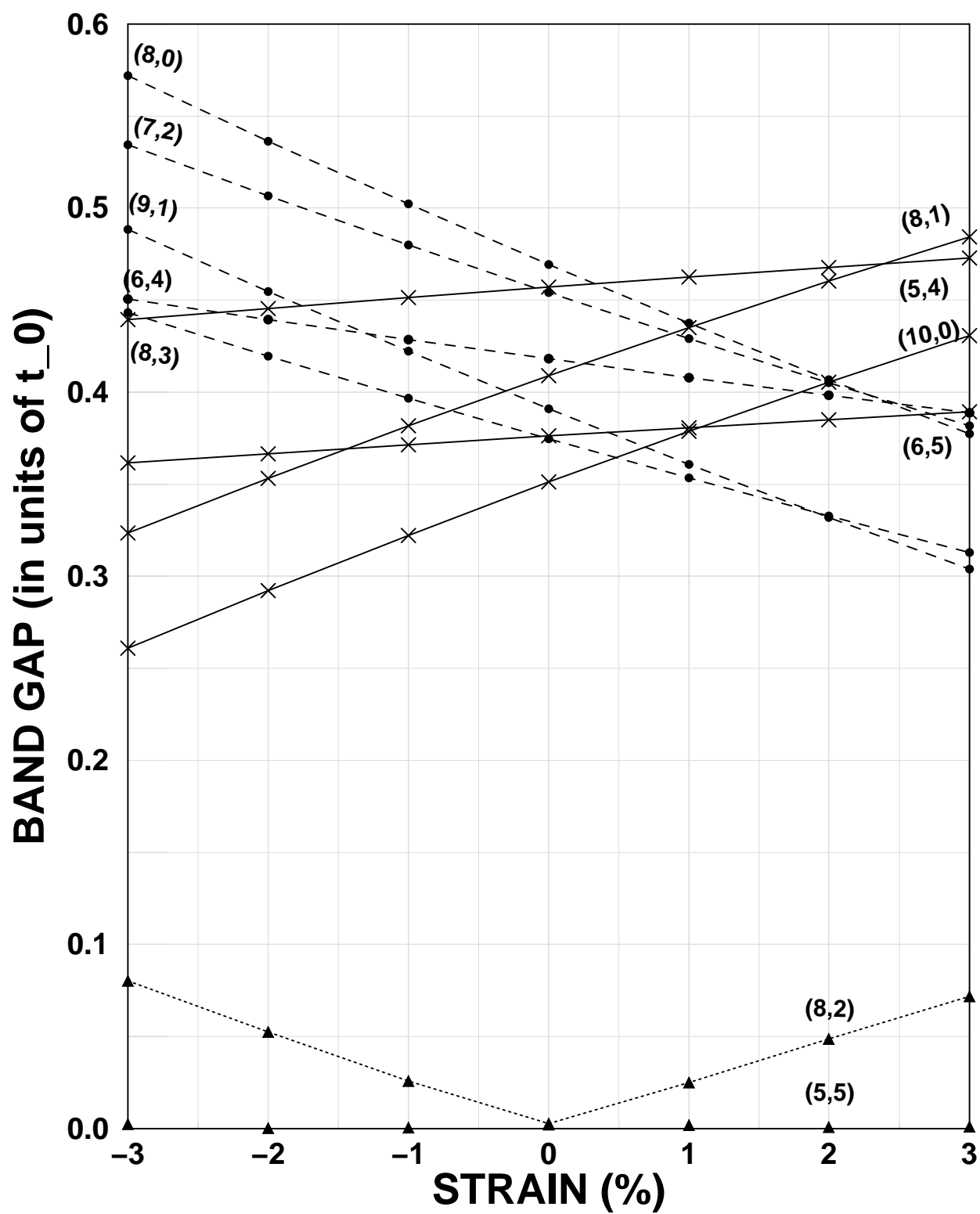


Fig. 2 / Yang

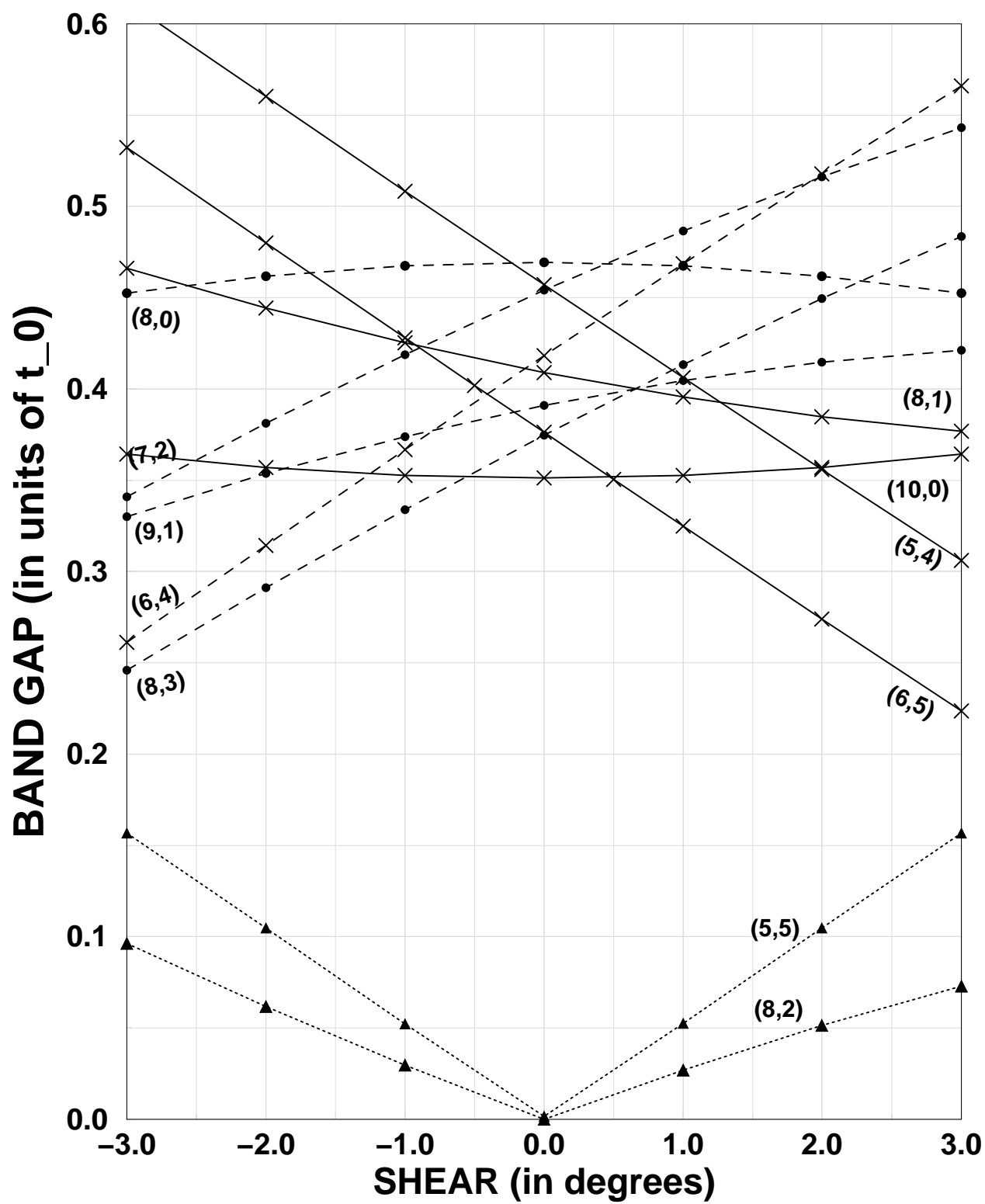


Fig. 3 / Yang

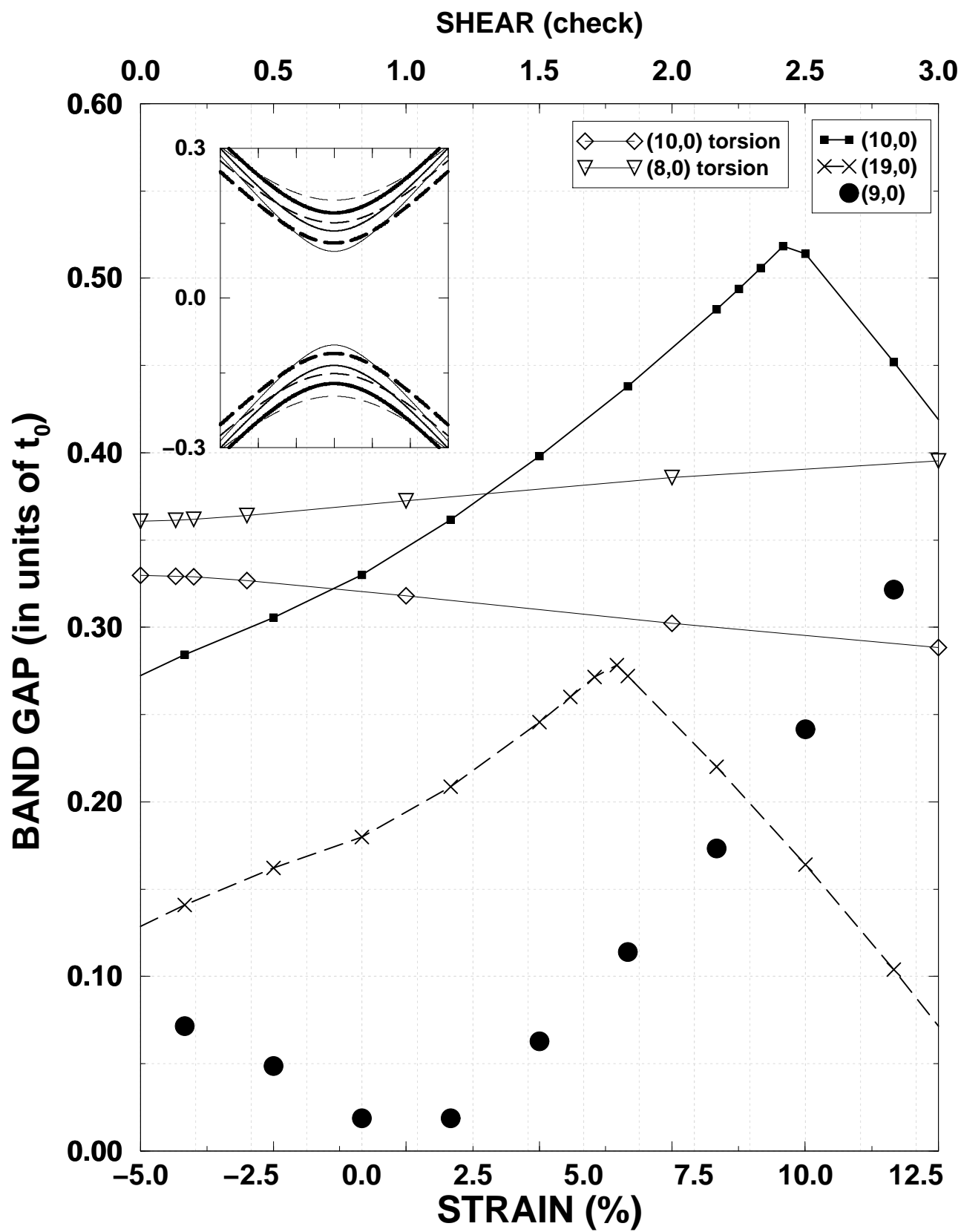


Fig. 4 / Yang